

Design of neural network-based control systems for active steering system

İkbal Eski · Ali Temürlenk

Received: 11 January 2013 / Accepted: 20 March 2013
© Springer Science+Business Media Dordrecht 2013

Abstract Nowadays, safety of road vehicles is an important issue due to the increasing road vehicle accidents. Passive safety system of the passenger vehicle is to minimize the damage to the driver and passenger of a road vehicle during an accident. Whereas an active steering system is to improve the response of the vehicle to the driver inputs even in adverse situations and thus avoid accidents. This paper presents a neural network-based robust control system design for the active steering system. Primarily, double-pinion steering system used modeling of the active steering system. Then four control structures are used to control prescribed random trajectories of the active steering system. These control structures are as classical PID Controller, Model-Based Neural Network Controller, Neural Network Predictive Controller and Robust Neural Network Predictive Control System. The results of the simulation showed that the proposed neural network-based robust control system had superior performance in adapting to large random disturbances.

Keywords Active steering system · Artificial neural network · Robust control · Random road input signal

1 Introduction

The active steering system plays a significant role in improving vehicle handling and stability. Several papers, a few of which are presented below, have been published in the area of the vehicle steering control system, vehicle stability and some of these papers are given below.

Zheng and Anwar researched a yaw stability control algorithm with active front wheel steering control of a vehicle [1]. The yaw stability control algorithm was obtained the decoupling of the lateral and yaw motion of a vehicle and the vehicle's yaw damping simultaneously by the feedback of both yaw rate and front steering angle. Also, the control system was applied on a steer-by-wire vehicle, and the benefits of the system were illustrated experimentally. A model of active steering approach for trajectory generation of unmanned ground vehicles were developed by Yoon et al. [2]. An optimal tracking problem was presented in the way of cost minimization under constraints. Simulation results show that the modified parallax method reflected the threat of the obstacles to the vehicle considering the dimension and state variables of the vehicle. An integrated control strategy presented for optimum coordination of individual

İ. Eski (✉)
Faculty of Engineering, Mechatronics Engineering
Department, Erciyes University, Kayseri 38039, Turkey
e-mail: ikbal@erciyes.edu.tr

A. Temürlenk
Faculty of Information Technologies and Engineering,
Ahmet Yesevi University, Turkestan city, Kazakhstan

brakes and front/rear steering subsystems [3]. A low-level slip-ratio controller has been designed to generate the desired longitudinal forces at small longitudinal slip-ratios, while averting wheel locking at large slip-ratios. The efficiency of the suggested approach was demonstrated through computer simulations.

Feedback linearization scheme for the control of vehicle's lateral dynamics was applied by Liaw and Chung [4]. Feedback linearization scheme was employed to construct the stabilizing control laws for the nominal model. The stability of the overall vehicle dynamics at the saddle node bifurcation was then guaranteed by applying the Lyapunov stability criterion. Since the remaining term of the vehicle dynamics contains the steering control input, which might change system equilibrium except the designed one. Parametric analysis of system equilibrium for an example vehicle model was also obtained to classify the regime of control gains for potential behavior of vehicle's dynamical behavior. A comparative study of different lateral controllers applied to the autonomous steering of automobiles was presented by Sotelo et al. [5]. The nonlinear nature of vehicle dynamics makes it a challenging problem in the intelligent transportation systems field, as long as a stable, accurate controller was compulsorily needed in order to ensure safety during navigation. The problem has been tackled under two different approaches. The first one was based on chained systems theory, while the second controller relied on fuzzy logic. A comparative analysis has been carried out based on the results achieved in practical trials.

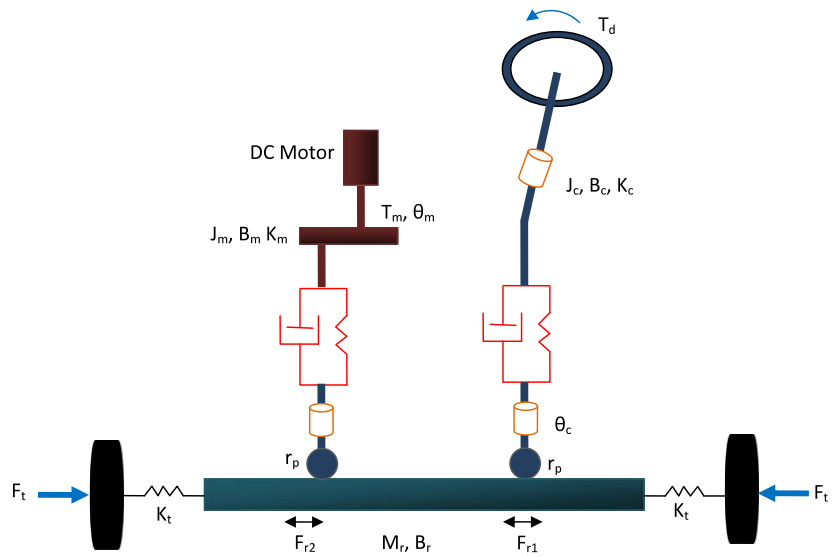
A kinematics model of planetary gear set and steering gear with active front steering system was installed by Gao and Wang [6]. Also, a controller of variable steering ratio for active front steering system was designed, and virtual road tests was made in CarMaker driver vehicle-road simulation environment. The results of simulation tests validated the controller performance and the advantage of variable steering ratio function. In addition, driving comfort was improved at low speed especially due to the active front steering system. Chu et al. [7] proposed coordinated control system to improve vehicle handling and stability by coordinating control of electronic stability program and active front steering. Primarily, they calculated the target yawing moment required to keep the vehicle stable according to PID control of the yaw-rate. Afterwards, they proposed a fuzzy method to control elec-

tronic stability program and active front steering. Finally, they used genetic algorithm to optimize the control rule to ensure the correctness and accuracy of the control rule. The performance of the integrated control system was evaluated by computer simulations at two different running condition and they compared the performance of the integrated system.

Fault detection of a steering wheel sensor signal in an active front steering system was researched by Malinen et al. [8]. A kinematics constraint, modeled as a dynamic system, was used to estimate the steering wheel angle. This estimated signal was compared with the measured signal. Using change detection algorithms typical failure patterns of the steering wheel sensor were detected quite easily. The estimated results and measurements from a prototype vehicle have been presented in this study. Escalona and Chamorro [9] researched a method for the stability analysis of the steady curving of vehicles based on equations of motion that were obtained using multi body dynamics. Owing to this method, steady circular motions could be described in terms of equilibrium points rather than periodic motions. Stability analyses were thus made much simpler and computationally efficient. Also, the method was applied to a simple wheeled mechanism. The numerical results thus obtained were consistent with those of analytical and classical theories, which testify to the accuracy of the proposed method. Jinlia et al. [10] proposed internal model control based on combined brake and front wheel active steering for vehicle stability control and compared with the four wheel steering internal model control.

Discrete neural control for flight path angle and velocity of a generic hypersonic flight vehicle was investigated by Xu et al. [11]. Primarily, strict-feedback form was set up for the attitude subsystem considering flight path angle, pitch angle, and pitch rate by altitude-flight path angle transformation. Secondly, the direct neural network control was proposed for attitude subsystem via back-stepping scheme. The direct design was employed for system uncertainty approximation with less online tuned neural network parameters and there was no need to know the information of the upper bound of control gain during the controller design. Similar neural network control was applied on velocity subsystem. Finally, the feasibility of the proposed controller was verified by a simulation example. A simple new method

Fig. 1 Schematic representation of the double-pinion steering system [20]



for dynamics of chaotic time continuous systems is proposed by Perc [12]. Determining the flexibility of regular and chaotic attractors is researched by Marhl and Perc [13]. They deploy a systematic approach, first introducing the simplest measure given by the local divergence of the system along the attractor, and then develop more rigorous mathematical tools for estimating the flexibility of the system's dynamics. A new method for controlling unstable periodic orbits is presented [14]. The effectiveness of the proposed method is shown on two different chaotic systems. Also, the chaotic behavior of a driven resonant circuit is researched [15] and their study used basic nonlinear time series analysis methods.

This paper is organized as follows: In Sect. 2, vehicle dynamic and kinematics model is presented. Our proposed control system is given in Sect. 3, and simulation results are presented in Sect. 4. Finally, conclusions are given Sect. 5.

2 Model of active steering system

The model of active steering system is composed of a double pinion rack mechanism, the primary mechanical steering system and an electric actuator motor additionally. Also, the electric actuator is connected to a different pinion gear with the steering rack [16], as illustrated in Fig. 1. The dynamics equations of the

model are given by

$$J_c \ddot{\theta}_c + B_c \dot{\theta}_c + K_c \left(\theta_c - \frac{X_r}{r_p} \right) = T_d \quad (1)$$

$$J_m \ddot{\theta}_m + B_m \dot{\theta}_m + K_m \left(\theta_m - \frac{X_r G}{r_p} \right) = T_m \quad (2)$$

$$\begin{aligned} M_r \ddot{X}_r + B_r \dot{X}_r + K_r X_r \\ = \frac{K_c}{r_p} \left(\theta_c - \frac{X_r}{r_p} \right) + \frac{K_m G}{r_p} \left(\theta_m - \frac{X_r G}{r_p} \right) + F_t \end{aligned} \quad (3)$$

where J_c and J_m represent the inertia moment of steering column and electric actuator, respectively. B_c , B_m and B_r represent the damping coefficient of steering column, electric actuator and steering rack. K_c , K_m and K_t denote the spring coefficient of steering column, electric actuator and tie/rack, respectively. θ_m and θ_c represent the angle of electric actuator and steering column, respectively. r_p is the rack radius, T_d is the driver torque, T_m is the torque of electric actuator, M_r is the rack mass, X_r is the displacement of rack, F_t is the lateral force from road and G is the motor gear ratio. The differential equations can be written in state-space notation when the state vector \mathbf{x} is defined as

$$\dot{\mathbf{x}} = \mathbf{A}\mathbf{x} + \mathbf{B}\mathbf{U} \quad (4)$$

$$\mathbf{y} = \mathbf{C}\mathbf{x} + \mathbf{D}\mathbf{U} \quad (5)$$

where \mathbf{y} is the output vector, \mathbf{U} is the input vector, \mathbf{A} is the state matrix, \mathbf{B} is the input matrix, \mathbf{C} is the output

matrix, **D** is the feed forward matrix. We have

$$\mathbf{A} = \begin{bmatrix} 0 & 1 & 0 & 0 & 0 & 0 \\ \frac{-K_c}{J_c} & \frac{-B_c}{J_c} & \frac{K_c}{J_c r_p} & 0 & 0 & 0 \\ 0 & 0 & 0 & 1 & 0 & 0 \\ \frac{K_c}{M_r r_p} & 0 & -\left(\frac{K_c + K_m G^2}{M_r r_p^2} + \frac{K_t}{M_r}\right) & \frac{-B_r}{M_r} & \frac{K_m G}{M_r r_p} & 0 \\ 0 & 0 & 0 & 0 & 0 & 1 \\ 0 & 0 & \frac{K_m G}{J_m r_p} & 0 & \frac{-K_m}{J_m} & \frac{-B_m}{J_m} \end{bmatrix} \tag{6}$$

$$\mathbf{B} = \begin{bmatrix} 0 & 0 \\ \frac{1}{J_c} & 0 \\ 0 & 0 \\ 0 & 0 \\ 0 & 0 \\ 0 & \frac{1}{J_m} \end{bmatrix} \tag{7}$$

$$\mathbf{C} = \left[0 \quad -K_m \quad \frac{-K_m G}{r_p} \quad 0 \quad K_m \quad 0 \right], \tag{8}$$

$$\mathbf{D} = [0 \quad 0]$$

$$\mathbf{x} = \begin{bmatrix} \theta_c \\ \dot{\theta}_c \\ \theta_m \\ \dot{\theta}_m \\ x_r \\ \dot{x}_r \end{bmatrix}, \quad \mathbf{y} = K_m \left(\theta_m - \frac{X_r G}{r_p} \right) = T_a \tag{9}$$

$$\mathbf{U} = \begin{bmatrix} T_d \\ u \end{bmatrix} \tag{10}$$

The geometric parameters of the active steering system are given in Table 1.

3 Control structures

In this study, four different control structures are used to control the active steering system. These control structures are as PID Controller, Model-Based Neural Network Controller, Neural Network Predictive Controller and Robust Neural Network Predictive Control System. Also, these control structures are given in sub sections.

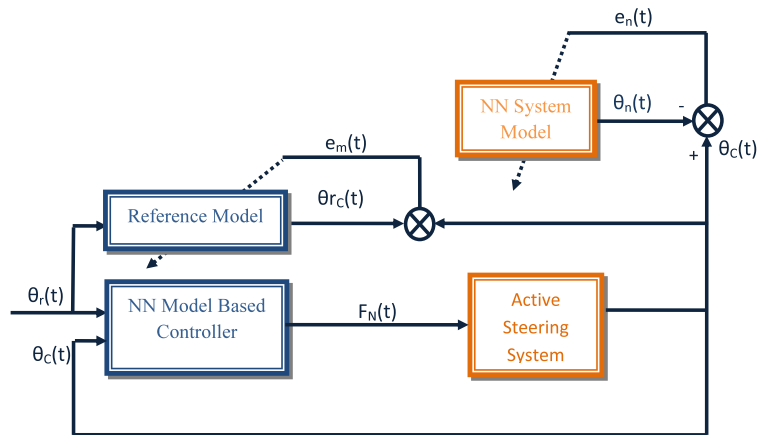
3.1 Model Based Neural Network Controller (MBNNC)

MBNNC structure uses two neural networks: a controller network and a plant model network, as shown in Fig. 2. The plant model network is a multi-layer neural network with a back-propagation learning scheme. The controller is a recurrent learning multi-layer neural network with “Plant Information” feedback along with other required feedback. The purpose of this controller is to provide the appropriate control action, given the current state of the system, in order to obtain a new state of the system such that the successive application of the control law drives the system toward a desired final state without violating the constraints imposed on the system and on the control variables.

Identification of the plant can be achieved by observing the input-output behavior of the plant. The plant model is used to generate the model error. Then the controller network is trained in such a way that the system response tracks the desired response (input to the model). Each of these networks has two layers with delayed inputs and outputs. The number of delays is proportional to the order of the system. The more the complexity of the system, the higher number of delays required. There is also flexibility so as to choose the number of hidden layers for each of these

Table 1 Active steering system parameters

Parameters	Value	Parameters	Value
B_c	0.0225 N m s/rad	J_m	4.52×10^{-4} kg m ²
B_r	3920 N m s/rad	K_c	172 N m/rad
B_m	3.34×10^{-3} N m s/rad	K_m	125 N m/rad
G	0.4686	K_t	23900 N m/rad
J_c	0.04 kg m ²	M_r	32 kg
r_p	0.0071 m		

Fig. 2 Model-based neural network controller


networks [17]. The MBNNC was designed to control the active steering system. It consisted of a third-order linear reference model and a neural network. The proposed neural controllers' law for active steering system is given by

$$F_N(t) = \sum_{j=1}^5 \left(\left(\frac{2}{(1 + e^{-2[\sum_{j=1}^5 [\theta_a(t)w_{1j}(t) + \theta_c(t)w_{2j}(t)] + 1])} - 1)} \right) \times w_{j1}(t) + 1 \right) \quad (11)$$

where $F_N(t)$ is the force of the NN controller, $\theta_a(t)$ is the desired angle input of the steering system for neural controller. $w_{1j}(t)$ is the weight matrices between first input layer neuron and in the hidden layer neurons. $w_{2j}(t)$ is the weight matrices between second input layer neuron and in the hidden layer neurons. $\theta_c(t)$ is the actual angle input of the steering system for neural controller.

3.2 Neural network predictive controller (NNPC)

There are typically two steps involved NNPC: system identification and control design. The system identification stage of NNPC is to train a neural network to present the forward dynamics of the plant. Figure 3 shows a schematic representation of the three layered feed forward neural network plant model. The prediction error between the plant output and the neural network output is used as the neural network training signal. The process is represented by Fig. 3. The neural

network plant model uses previous plant inputs and previous plant outputs to predict future values of the plant output [18]. In the control stage, the plant model is used by the controller to predict future performance. The neural network model predicts the plant response. We have

$$F_N(t) = \sum_{j=1}^5 f(\theta_a(t+j) - \theta_n(t+j))^2 + \rho \sum_{j=1}^2 g(F'_N(t+j-1) - F'_N(t+j-2))^2 \quad (12)$$

where f and g are activation functions of the hidden layer and the output layer, respectively, as follows:

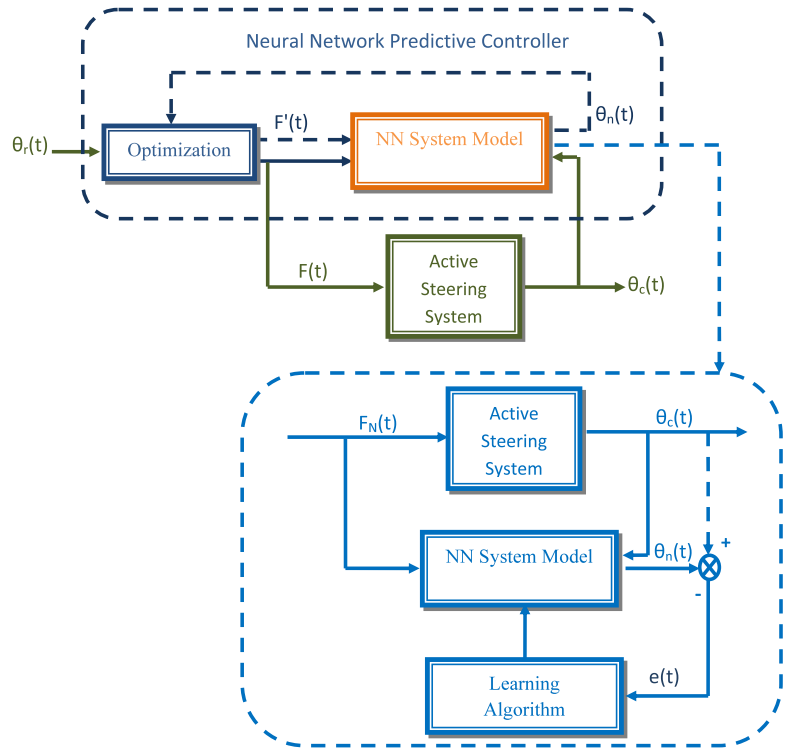
$$f(t) = \tan \text{sig}(t) = \frac{2}{(1 + e^{-2t})} - 1, \quad g(t) = t$$

The $F'_N(t)$ variable is the tentative control signal, $\theta_a(t)$ is the desired output, $\theta_n(t)$ is the neural network model output. The ρ value determines the contribution that the sum of the squares of the control increments provides for the performance index. The optimization block determines the control input that optimizes plant performance over a finite time horizon.

3.3 Robust neural feedback control system (RNFCFS)

A designed control system is employed to control the active steering system. The purpose of this proposed

Fig. 3 Neural network predictive controller



control system is to provide the appropriate control action. The mathematical expression of the force of the RNF control system is given by

$$\begin{aligned}
 F(t) = & \sum_{j=1}^5 f(\theta_a(t+j) - \theta_n(t+j))^2 \\
 & + \rho \sum_{j=1}^2 g(F'_N(t+j-1) - F'_N(t+j-2))^2 \\
 & + \sigma e^{-\beta t}
 \end{aligned}
 \tag{13}$$

where σ and β are the robust controller parameters and are empirically set to $\sigma = 100$ and $\beta = 0.0001$. Schematic representation the proposed neural based control system model is shown in Fig. 4. The Levenberg–Marquardt algorithm is used to adjust the weights of neural network.

3.4 Resilient backpropagation algorithm (RPROP)

The Resilient Backpropagation algorithm is a local adaptive learning scheme, performing supervised batch learning in feed-forward neural networks [19].

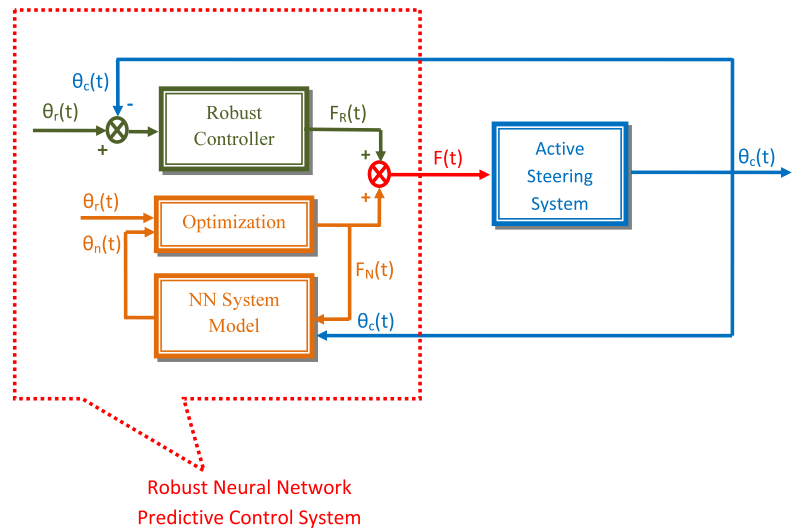
The basic principle of this algorithm is to eliminate the harmful influence of the size of the partial derivative’s size on the weight step. As a consequence, only the sign of the derivative is considered to indicate the direction of the weight update. This algorithm typically uses a sigmoid function in the hidden layer and a linear function in the output layer. Here, w_{ij} is the weight matrix, $\Delta_{ij}(t)$ is the update value for each weight. A second learning rule is introduced which determines the evolution of the update value $\Delta_{ij}(t)$. This estimation is based on the observed behavior of the partial derivative during two successive weight-steps:

$$\Delta_{ij}(t) = \begin{cases} \lambda^+ \Delta_{ij}(t-1), & \text{if } \frac{\partial E}{\partial w_{ij}}(t) \frac{\partial E}{\partial w_{ij}}(t-1) > 0 \\ \lambda^- \Delta_{ij}(t-1), & \text{if } \frac{\partial E}{\partial w_{ij}}(t) \frac{\partial E}{\partial w_{ij}}(t-1) < 0 \\ \Delta_{ij}(t-1), & \text{else} \end{cases}
 \tag{14}$$

where

$$0 < \lambda^- < 1 < \lambda^+.
 \tag{15}$$

Fig. 4 Robust neural network predictive control system



The adaptation rule works in the following way. Every time the partial derivative of the corresponding weight w_{ij} changes its sign, which indicates that the last update was too big and the algorithm has jumped over a local minimum, the update value $\Delta_{ij}(t)$ is decreased by the factor λ^- . If the derivative retains its sign, the update value is slightly increased in order to accelerate convergence in shallow regions. Once the update value for each weight is adapted, the weight-update itself follows a very simple rule: if the derivative is positive (increasing error), the weight is decreased by its update-value, if the derivative is negative, the update value is added:

$$\Delta w_{ij}(t) = \begin{cases} -\Delta_{ij}(t), & \text{if } \frac{\partial E}{\partial w_{ij}}(t) > 0 \\ \Delta_{ij}(t), & \text{if } \frac{\partial E}{\partial w_{ij}}(t) < 0 \\ 0, & \text{else} \end{cases} \quad (16)$$

$$w_{ij}(t + 1) = w_{ij}(t) + \Delta w_{ij}(t) \quad (17)$$

However, there is one exception. If the partial derivative changes sign, i.e. the previous step is too large and the minimum is missed, the previous weight-update is reverted:

$$\Delta w_{ij}(t) = -\Delta w_{ij}(t - 1), \quad \text{if } \frac{\partial E}{\partial w_{ij}}(t) \frac{\partial E}{\partial w_{ij}}(t - 1) < 0 \quad (18)$$

Due to that ‘backtracking’ weight-step, the derivative is supposed to change its sign once again in the following step. In order to avoid a double punishment of the updatevalue, there should be no adaptation of the update-value in the succeeding step. In practice this can be done by setting $\frac{\partial E}{\partial w_{ij}}(t - 1) = 0$ in the Δ_{ij} update rule above. The partial derivative of the total error is given by

$$\frac{\partial E}{\partial w_{ij}}(t) = \frac{1}{2} \sum_{p=1}^P \frac{\partial E_p}{\partial w_{ij}}(t) \quad (19)$$

Hence, the partial derivatives of the errors must be accumulated for all P training patterns. This means that the weights are updated only after the presentation of all training patterns. α (weight-decay) parameter determines the relationship of two goals, namely to reduce the output error (the standard goal) and to reduce the size of weights (to improve generalization). The composite error function is

$$E = \frac{1}{2} \sum_{p=1}^P \sum_{j=1}^{N_o} (d_{pj} - e_{pj})^2 + \frac{1}{10^\alpha} \sum_{i,j} w_{ij}^2 \quad (20)$$

Moreover, for comparison purposes, the classical PID controller was used for trajectory control active steering system. The PID controller was initially tuned using the Ziegler-Nichols method, and the PID parameters are $K_P = 60$, $K_I = 7200$ and $K_D = 1$.

4 Simulation results

This section presents simulation result of the active steering system for random input signals using the PID controller, the MBNNC, the NNPC and the RNNPC approaches. The first structure used in the control of active steering system is the PID controller. The simulation results and the values of error obtained from the random input signal of this organ have been presented in Fig. 5. As is seen in the figure, the PID controller is unable to adapt itself to random input signal, which changes suddenly, but it can follow the input signal after a certain period. In this case the PID controller, as such it is, is hardly adequate to run active steering system (Figs. 5b and 5d).

The second structure employed to control the system, however, is the MBNNC approach. The study of Figs. 6a–6d will reveal that the values of error at the points of sudden change resulting from the characteristic reference input signal is higher than that in the PID controller. In addition, the MBNNCA structure has yielded the poorest results among the other neural network structure employed in the control of the active steering system. The reason for this is that the reference model error used in the MBNNCA approach is high and that the learning algorithm used in arranging the weights of the control structure to reduce this error has remained inadequate.

The third structure employed in simulation is the NNPC structure. The results and error values for two

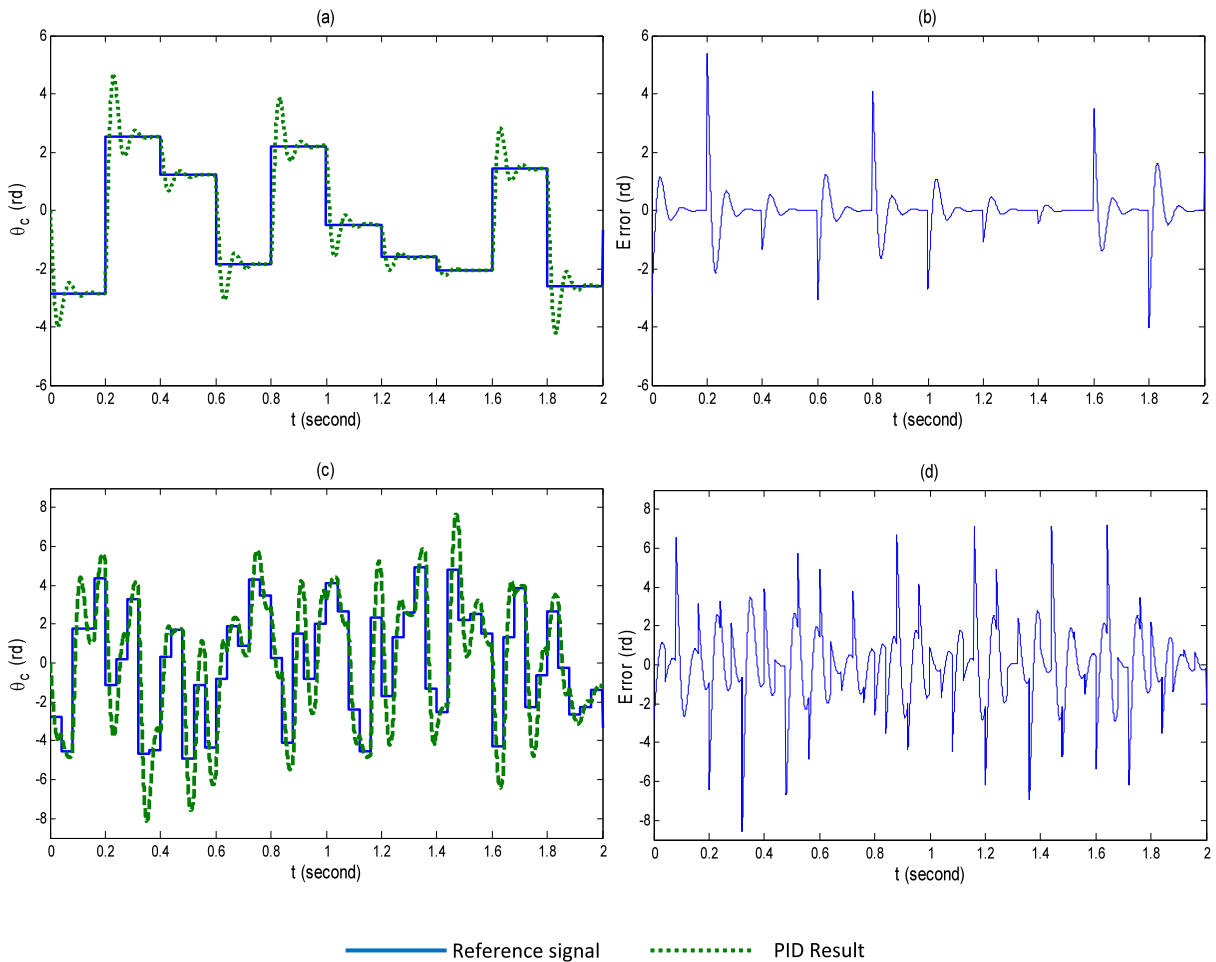


Fig. 5 Variations of the steering column angle using the PID Controller. (a) Random1 input signal. (b) Error of the PID Controller. (c) Random2 input signal. (d) Error of the PID Controller

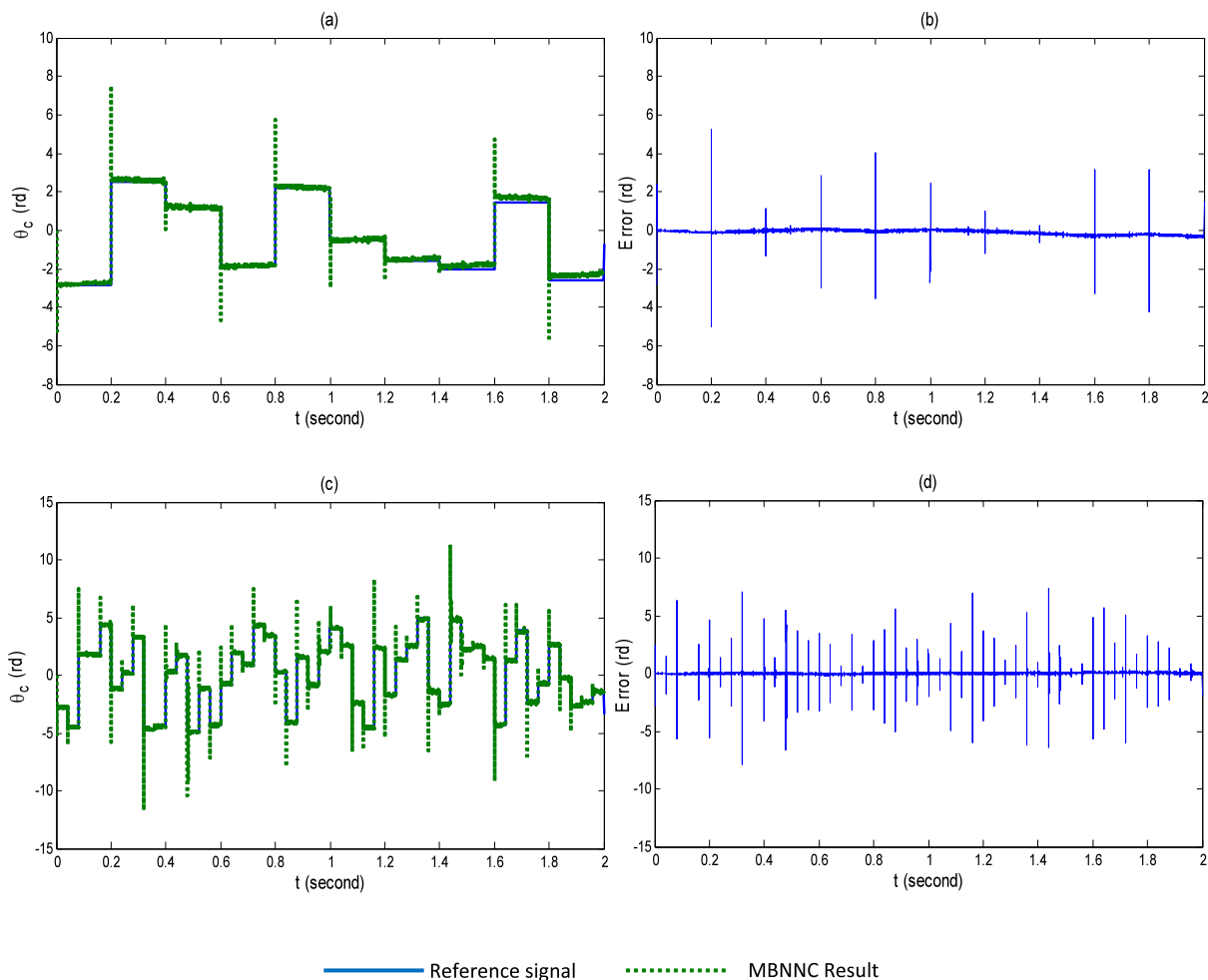


Fig. 6 Variations of the steering column angle using the MBNN Controller. (a) Random1 input signal. (b) Error of the MBNN Controller. (c) Random2 input signal. (d) Error of the MBNN Controller

different random input signals have been presented in Fig. 7. The analysis of the graphics has revealed that the NNPC approach has yielded far more favorable results compared to other three controllers. The NNPC approach adapts itself to sudden changes of random input signal far more favorably and it has been observed that there have been considerable reductions in steady state errors. The reason for this superior performance is that the neural network model uses optimization algorithm while being constituted. The difference between the output signal of neural network model and active steering system, i.e. error is used for the adjustment of the parameters of optimization algorithm.

In addition, the values of error between the output signal of neural network model and the output signal

of the controlled system in the system identification section of this controller are used for the adjustment of the weights in the learning algorithm of the NNPC. Therefore, the current NNPC approach to the control of active steering system is more appropriate than, but inadequate compared to, other control structures. For this reason, a controller with a robust constitution capable of both being adapted to sudden changes of the random input signal and of eliminating the steady state errors constantly has been added to the NNPC structure to constitute the neural network-based robust control system.

The response of developed RNNP to random input signal and its error values have been given in Fig. 8. The values of error at sudden change points for

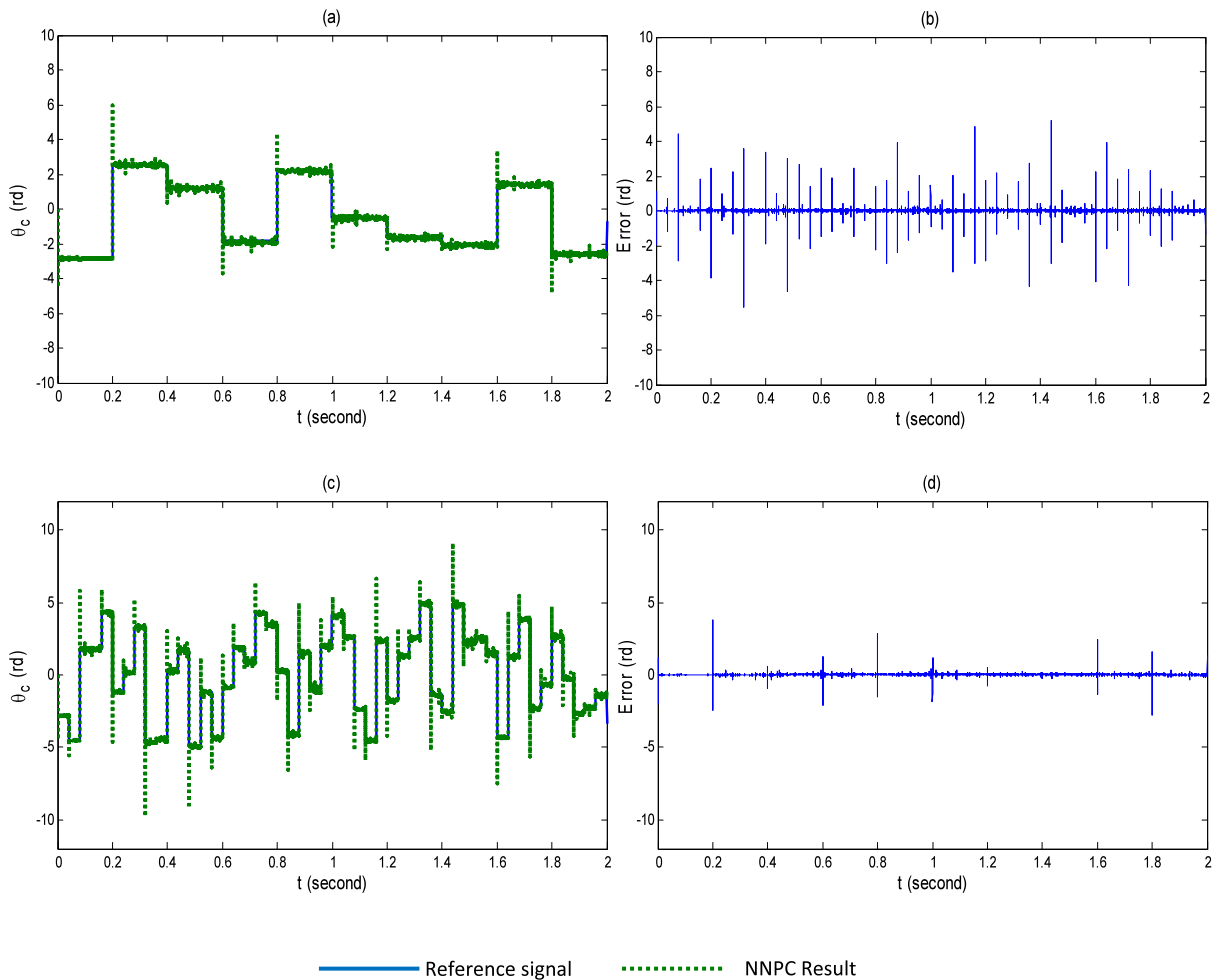


Fig. 7 Variations of the steering column angle using the NNP Controller. (a) Random1 input signal. (b) Error of the NNP Controller. (c) Random2 input signal. (d) Error of the NNP Controller

two different random input signals are considerably low as compared to those for the other three control structures. Moreover, the system does not have steady state errors. Since the robust structure of the proposed control system constantly reduces the errors exponentially, it has yielded more favorable results in a short time than the controllers. For all these reasons, the suggested neural network-based robust control system is the most appropriate approach for the control of active steering system.

5 Conclusions

In this study, the control of the active steering system is used in four different control structures. Except for the

classical PID controller, neural network is based on all the other control structures. The reason for preferring the neural network approach for controlling the system is its ability to learn, their high-speed performance owing to their parallel structures, their non-linearity, and their ability to generalize. Moreover, for comparison purposes, the classical PID controller was used for random trajectory control active steering system. It has been observed that the PID controller is not suitable for the control of such systems since it cannot adapt itself to sudden changes in random input signals because of their control parameters being constant. Also, in the current study, in order to test performance of the controllers, two different random signals are used as input signal. Within used neural network-based con-

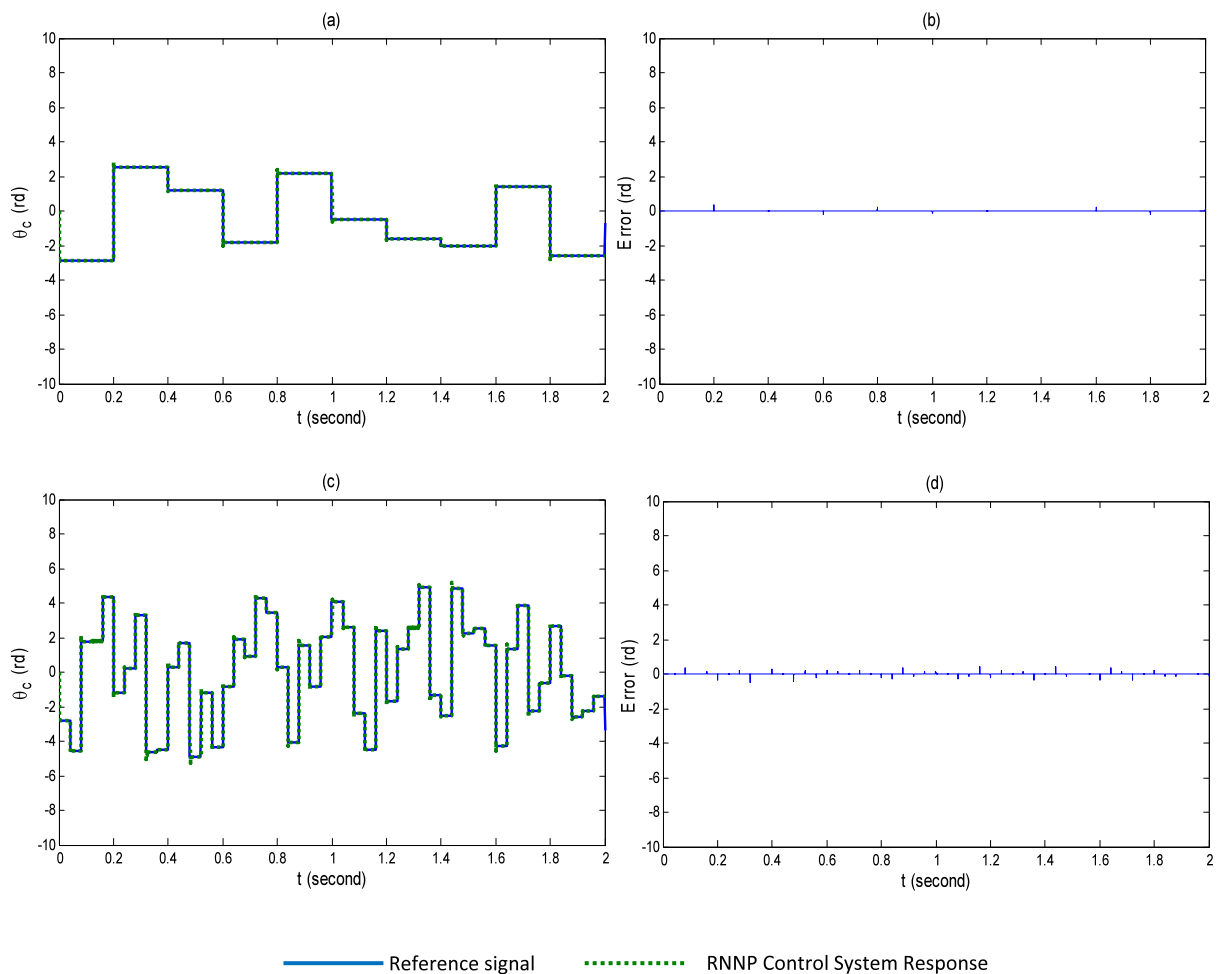


Fig. 8 Variations of the steering column angle using the RNNP Control System. **(a)** Random1 input signal. **(b)** Error of the RNNP Control System. **(c)** Random2 input signal. **(d)** Error of the RNNP Control System

troller, the NNPC approach has given the best result. So, this neural network structure is used for the proposed robust control system. From the evaluation of the obtained simulation results, the proposed neural based control system is suitable for the control of such systems. In addition, the developed neural based robust control system, which can be applied to any vehicle system, will contribute to the research in this field in automotive manufacturing sector.

References

- Zheng, B., Anwar, S.: Yaw stability control of a steer-by-wire equipped vehicle via active front wheel steering. *Mechatronics* **19**, 799–804 (2009)
- Yoon, Y., Shin, J., Kim, H.J., Park, Y., Sastry, S.: Model-predictive active steering and obstacle avoidance for autonomous ground vehicles. *Control Eng. Pract.* **17**, 741–750 (2009)
- Tavasoli, A., Naraghi, M., Shakeri, H.: Optimized coordination of brakes and active steering for a 4WS passenger car. *ISA Trans.* **51**, 573–583 (2012)
- Liaw, D.C., Chung, W.C.: A feedback linearization design for the control of vehicle's lateral dynamics. *Nonlinear Dyn.* **52**, 313–329 (2008)
- Sotelo, M.A., Naranjo, E., Garcia, R., Pedro, T., Carlos, G.: Comparative study of chained systems theory and fuzzy logic as a solution for the nonlinear lateral control of a road vehicle. *Nonlinear Dyn.* **49**, 463–474 (2007)
- Gao, Z., Wang, J., Wang, D.: Dynamic modeling and steering performance analysis of active front steering system. *Proc. Eng.* **15**, 1030–1035 (2011)
- Chu, L., Gao, X., Guo, J., Liu, H., Chao, L., Shang, M.: Coordinated control of electronic stability program and ac-

- tive front steering. *Procedia Environ. Sci.* **12**, 1379–1386 (2012)
8. Malinen, S., Lundquist, C., Reinelt, W.: Fault detection of a steering wheel sensor signal in an active front steering system. In: *IFAC Symp. Series*, pp. 510–515 (2006)
 9. Escalona, J.L., Chamorro, R.: Stability analysis of vehicles on circular motions using multibody dynamics. *Nonlinear Dyn.* **53**, 237–250 (2008)
 10. Jinlai, M., Bofu, W., Jie, C.: Comparisons of 4WS and Brake-FAS based on IMC for vehicle stability control. *J. Mech. Sci. Technol.* **25**, 1265–1277 (2011)
 11. Xu, B., Wang, D., Sun, F., Shi, Z.: Direct neural discrete control of hypersonic flight vehicle. *Nonlinear Dyn.* **70**, 269–278 (2012)
 12. Perc, M.: Visualizing the attraction of strange attractors. *Eur. J. Phys.* **26**, 579–587 (2005)
 13. Marhl, M., Perc, M.: Determining the flexibility of regular and chaotic attractors. *Chaos Solitons Fractals* **28**, 822–833 (2006)
 14. Perc, M., Marhl, M.: Detecting and controlling unstable periodic orbits that are not part of a chaotic attractor. *Phys. Rev. E* **70**, 016204 (2004)
 15. Kodba, S., Perc, M., Marhl, M.: Detecting chaos from a time series. *Eur. J. Phys.* **26**, 205–215 (2005)
 16. Güvenç, L., Ersolmaz, S.S., Öztürk, E.S., Çetin, E., Kılıç, N., Güngör, S., Kanbolat, A.: Stability enhancement of a light commercial vehicle using active steering. *SAE Inc.*, pp. 107–120 (2006)
 17. Yıldırım, Ş., Eski, İ.: Design of robust model based neural controller for controlling vibration of active suspension system. *J. Sci. Ind. Res.* **65**, 646–654 (2006)
 18. Eski, İ., Yıldırım, Ş.: Vibration control of vehicle active suspension system using a new robust neural network control system. *Simul. Model. Pract. Theory* **17**, 778–793 (2009)
 19. Riedmiller, M., Braun, H.: A direct adaptive method for faster backpropagation learning: the RPROP algorithm. In: *ICNN, San Francisco, USA*, pp. 586–591 (1993)
 20. Öncü, S., Karaman, S., Güvenç, L., Ersolmaz, S., Öztürk, E., Çetin, E., Sinal, M.: Robust yaw stability controller design for a light commercial vehicle using a hardware in the loop steering test rig. In: *IEEE Int. Veh. Sym, Istanbul* (2007)